

Temperature, Pressure, and Concentration Dependence of the Osmotic Pressure of Dilute He³-He⁴ Mixtures*

J. Landau, J. T. Tough, N. R. Brubaker, and D. O. Edwards

Physics Department, The Ohio State University, Columbus, Ohio 43210

(Received 22 May 1970)

The osmotic pressure of He³-He⁴ mixtures has been measured at temperatures 0.027–0.65 K, for concentrations up to 10-mole % He³, and for hydrostatic pressures of 0.26, 10, and 20 atm. The osmotic pressure was measured directly with a sensitive specially designed diaphragm pressure gauge. The temperature and concentration dependence of the osmotic pressure is in fair agreement with the effective interaction theory proposed by Bardeen, Baym, and Pines (BBP). It also agrees with a simple empirical model which avoids the complicated calculations involved in obtaining the thermodynamic properties at finite temperatures from the BBP theory. The model fits the temperature dependence of other thermodynamic properties of solutions. The osmotic pressure at absolute zero at 10 and 20 atm is used to determine the He³ effective mass and somewhat speculative values of the BBP quasiparticle interaction $V(k)$ under pressure. The interaction under pressure is found to have a minimum at a nonzero value of k , and it may give rise to a "supermobile" transition at comparatively high temperatures.

I. INTRODUCTION

Measurements of the osmotic pressure of dilute He³-He⁴ mixtures are useful in understanding the thermodynamic properties of this quantum liquid in the fully degenerate^{1,2} and semiclassical²⁻⁴ regions. The present measurements cover the temperature range 0.027–0.65 K spanning a wide degree of degeneracy. In addition, the measurements have been made under pressures of 0.26, 10, and 20 atm, allowing examination of the pressure dependence of the mixture properties. In an earlier brief paper¹ we discussed the osmotic pressure at 0 K and zero pressure and some results on the maximum solubility of He³. The present paper is mainly concerned with the experimental method, a complete presentation of the experimental results, and a comparison with theory at finite temperatures and pressures.

At temperatures below ~0.6 K the density of phonons and rotons in liquid helium becomes negligibly small and the He⁴ atoms act only as a superfluid background for the He³ atoms. In the model of Landau and Pomeranchuk⁵ in this temperature region, the excited states of the mixture are due entirely to He³ quasiparticles (of number equal to the He³ atoms) with the energy-momentum relation

$$\epsilon = -E_3 + p^2/2m^* . \quad (1)$$

Here E_3 is the binding energy of a single He³ atom in He⁴ and m^* is the effective mass of a quasiparticle. Specific-heat⁶ and second-sound data⁷⁻¹⁰ indicate that m^* is approximately 2.4 times the bare He³ mass (m_3) in mixtures where the He³ mole fraction X is small. Measurements under pressure show that m^*/m_3 increases with P . The binding energy has been deduced from heat of mixing data¹¹ to be

$E_3/k_B = 2.785 \pm 0.011$ K at $P=0$. The collective behavior of the quasiparticles is that of a Fermi gas with degeneracy temperature T_F given by

$$k_B T_F = \hbar^2 k_F^2 / 2m^* = (\hbar^2 / 2m^*) (3\pi^2 n_3)^{2/3} , \quad (2)$$

where n_3 is the He³ number density. The gas of quasiparticles exerts a pressure corresponding to the average rate of momentum transfer per unit area. This pressure is approximately the osmotic pressure of the He³ in solution. The thermodynamic definition of the osmotic pressure can be obtained by considering two chambers maintained at a temperature T below the helium λ point. The chambers are connected by an ideal superleak (completely permeable to superfluid He⁴ and impermeable to He³). One chamber is completely filled with pure He⁴, the other with a He³-He⁴ mixture at pressure P and mole fraction X . We define the osmotic pressure $\pi(P, T, X)$, so that in equilibrium, the pressure in the pure He⁴ is $P - \pi$. Since the He⁴ chemical potential is the same in both chambers,¹² we obtain

$$\mu_4(P, T, X) = \mu_4(P - \pi, T, 0) . \quad (3)$$

Expanding the right-hand side of Eq. (3) as a Taylor series about the point $(P, T, 0)$ gives

$$\mu_4(P, T, X) = \mu_4(P, T, 0) - \pi(P, T, X) v_4 - \frac{1}{2} \pi^2 v_4 \kappa_4 + \dots , \quad (4)$$

where

$$v_4(P, T) = \frac{\partial \mu_4(P, T, 0)}{\partial P} ,$$

$$\kappa_4 = - \frac{1}{v_4} \frac{\partial v_4}{\partial P}$$

are the molar volume and isothermal compressibility of pure He^4 . For the range of the present data, the third term in Eq. (4) is negligible compared to the second, and succeeding terms in the series are smaller yet. We therefore adopt as a working definition of the osmotic pressure

$$\pi(P, T, X) v_4(P, T) = \mu_4(P, T, 0) - \mu_4(P, T, X). \quad (5)$$

In the simple Landau-Pomeranchuk model of mixtures where $X \ll 1$, the osmotic pressure π is just the pressure of an ideal Fermi gas $\pi v_4 = \frac{2}{3} X U_F$, where $U_F(T, T_F)$ is the ideal-gas internal energy. Including the empirical result that the molar volume of a solution depends on the concentration according to the equation

$$v(P, T, X) = v_4[1 + X\alpha(P, T, X)]$$

requires the addition of a small correction term μ_α to $\frac{2}{3} X U_F$.

Bardeen, Baym, and Pines (BBP)¹³ extended the Landau-Pomeranchuk model to finite concentrations by including an effective interaction between the quasiparticles. The Fourier transform of the interaction $V(k)$ describing the scattering of two He^3 quasiparticles with momentum transfer k has been determined up to $k \approx 0.6 \text{ \AA}^{-1}$ from the low-temperature transport properties.^{6,14} The original $V(k)$ of BBP and a later version proposed by Baym and Ebner¹⁵ both suffered from the use of approximate solutions to the Boltzmann equation for the transport coefficients. Ebner recently¹⁶ gave an "optimum" $V(k)$ based upon exact solutions to the Boltzmann equation. He also^{17,18} used high-temperature spin-diffusion⁶ data to extend $V(k)$ up to $k \approx 1.5 \text{ \AA}^{-1}$. When the interaction between quasiparticles is included, the osmotic pressure is increased by another term π_{int} , so that

$$\pi(P, T, X) v_4 = \frac{2}{3} X U_F(T, T_F) + \mu_\alpha + \pi_{\text{int}} v_4. \quad (6)$$

Since the first two terms can be calculated to within the uncertainty of m^* , measurements of the osmotic pressure give values of π_{int} which can be compared with values calculated from $V(k)$. Such a comparison (for $P=0$) in the high-temperature ($T > T_F$) region previously gave unsatisfactory agreement,^{3,4} while at $T=0$ the agreement¹ is within 10–20% in $V(k)$. In this paper we make a new comparison with theory over the whole temperature range. An alternative approach is to use the empirical values of π_{int} to obtain a potential $V(k)$. In this way the present data are used to deduce $V(k)$ at pressures other than zero.

II. APPARATUS

The apparatus is shown schematically in Fig. 1. The experimental cell, made of Epibond 100 A,¹⁹ contained two chambers, each with a filling capillary: one for the He^3 - He^4 mixture and one for pure

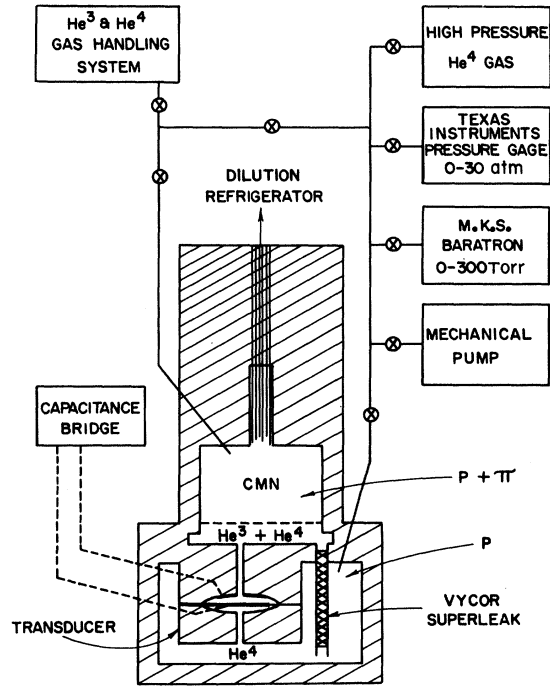


FIG. 1. Schematic drawing of osmotic pressure apparatus.

He^4 . The mixture chamber contained a cerium magnesium nitrate (CMN) thermometer and communicated with the pure- He^4 chamber through a Vycor glass superleak.²⁰ The differential pressure across the superleak, the osmotic pressure π , was measured with a specially designed diaphragm pressure transducer, which transformed a change in π into a change of capacitance. The capacitance was measured with a General Radio 1615-A bridge. This system, which we described in another paper,²¹ resolved changes of 10^{-3} Torr in the differential pressure.

The experimental chambers were pressurized through the He^4 filling capillary with He^4 from an external high-pressure gas source. The pressure in the cell could thus be varied without changing the He^3 number density. External pressure gauges were used to measure the ambient pressure in the cell.

The mixture of He^3 and He^4 was cooled by a brush of 10 000 #50 copper wires which were hard soldered to a thermal connector²² on a dilution refrigerator. The mixture chamber of the cell contained an electric heater. Electrical leads for the heater and the transducer, as well as the filling capillaries, were sealed through the cell walls by means of Epibond 121.

The magnetic susceptibility of the cylinder (diameter equal to height) of 5 g of powdered CMN was used as a primary thermometer. The magnetic

temperature, calculated from the Curie law, is known to be insignificantly different from the absolute temperature above 0.01 K.²³ The susceptibility was determined by measuring the change in mutual inductance of two coils which were located on the outside of the refrigerator vacuum jacket. At the beginning of each experiment the CMN was calibrated against the vapor pressure of the He⁴ bath between 1 K and the λ point.

Since the experiments were performed at known pressures with measured amounts of He³, it was only necessary to determine the volume of the mixture chamber of the cell in order to obtain the mixture concentration. An external standard volume and a manometer were used to measure the amount of He⁴ gas needed to completely fill the chamber with liquid helium at a temperature above the λ point. The same system was also used to add measured quantities of He³ throughout the experiment.

At the beginning of each experiment the transducer was calibrated against the absolute osmotic pressure measurements of Wilson *et al.* at 0.65 K.^{3,4} The calibration was done at the standard temperature and external pressure $T_s = 0.65$ K, $P_s = 0.26$ atm. The He³ concentration was increased from zero in approximately 0.35% steps (corresponding to approximately 5-Torr increments in π) to $X \approx 2\%$ ($\pi \approx 30$ Torr). The capacitance at each concentration was changed not only by the deflection of the transducer diaphragm due to π , but also by the changing dielectric constant of the mixture. Also, because measurements were made at $T \leq T_s$ and $P \geq P_s$, it was important to identify a calibration function which was a function of π only and which eliminated the effects of temperature and ambient pressure. This was done with the aid of a physical model of the capacitor consisting of a π -dependent capacitor in parallel with a π -independent fringe capacitance.²¹ On the assumption that the fraction of space in each capacitor filled with helium mix-

ture (filling factor γ) is the same (this assumption introduces negligible error), it follows that the desired calibration function is

$$\Delta C = \left(C_s - \frac{C}{(1 + \gamma\delta)F(T, P)} \right) \frac{1 + \delta}{1 + \gamma\delta}. \quad (7)$$

Here $C = C(\pi, P, T, X)$ is the measured capacitance and $C_s = C(0, P_s, T_s, 0)$. The denominator under C reduces it to standard conditions, since δ is defined so that the dielectric constant of the mixture is $\epsilon = \epsilon_s(1 + \delta)$. The weak temperature and pressure dependence of the construction materials (Mylar and Epibond) is represented by the dimensionless function $F(T, P)$. By measuring C at 2 K and $P = P_s$ with the capacitor both empty and filled with He⁴, we found γ to be 0.685. The function F was represented by

$$F(T, P) = 1 + F_1(T) + F_2(P),$$

with $F_1(T_s) \equiv F_2(P_s) \equiv 0$. The corrections introduced by δ and $F(T, P)$ were quite small. The maximum values of these quantities encountered in the experiments were $\delta \approx 0.01$, $F_1(T) \approx 10^{-4}$, and $F_2(P) \approx 2 \times 10^{-3}$. Careful analysis demonstrated that to a very good approximation ΔC depended only on π .

The largest source of error in the data is the 1% systematic uncertainty which we accept by calibrating against the osmotic pressure measurements of Wilson *et al.*^{3,4} In addition, there is a 0.7% systematic uncertainty in the measurement of the He³ concentration and a 0.4% random uncertainty in the measurement of π . As we explain in Sec. III, the present data were fitted to a simple thermodynamic model which can be used to compute the osmotic pressure at any temperature and concentration. The osmotic pressure at 0.32 K was calculated in this way and compared with the data of Wilson *et al.*^{3,4} at the same temperature. The calculated results fell about 2% below the Wilson *et al.* values. We believe this is the re-

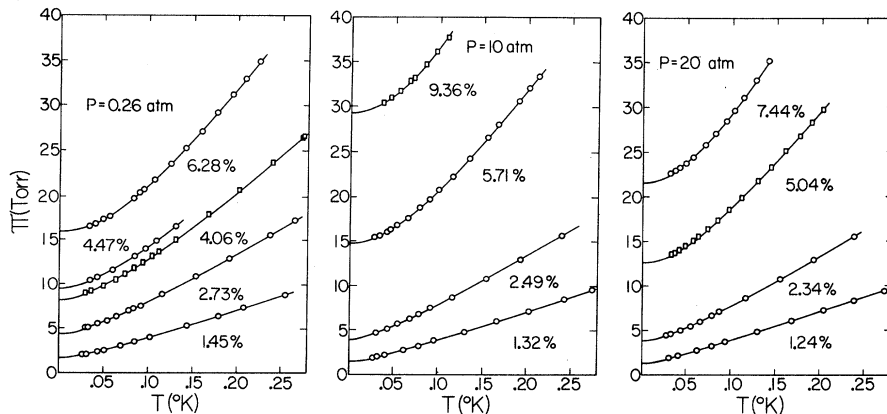


FIG. 2. Osmotic pressure as a function of temperature at various concentrations and pressures. Circles and squares represent data taken on two distinct runs and are given in Table I. Solid lines are the empirical fit to data discussed in Sec. III B.

TABLE I. The osmotic pressure of single-phase He³-He⁴ solutions at pressures of 0.26, 10, and 20 atm, and at various temperatures and concentrations. These data are also shown in Fig. 2.

$P=0.26$ atm									
$X=1.449\%$		$X=2.73\%$		$X=4.06\%$		$X=4.47\%$		$X=6.28\%$	
T	π	T	π	T	π	T	π	T	π
0.027	1.98	0.030	5.02	0.031	8.86	0.044	10.63	0.034	16.28
0.032	2.08	0.033	5.08	0.036	9.04	0.060	11.46	0.041	16.56
0.044	2.34	0.044	5.41	0.051	9.62	0.060	11.44	0.050	17.01
0.052	2.52	0.055	5.83	0.051	9.64	0.086	13.01	0.058	17.46
0.069	2.98	0.066	6.27	0.064	10.32	0.098	13.86	0.084	19.39
0.086	3.44	0.079	6.88	0.075	10.91	0.110	14.69	0.090	20.06
0.103	3.95	0.085	7.13	0.085	11.56			0.095	20.38
0.145	5.21	0.087	7.25	0.094	12.15			0.108	21.49
0.179	6.30	0.092	7.50	0.104	12.84			0.126	23.20
0.180	6.29	0.094	7.57	0.112	13.37			0.142	24.93
0.208	7.17	0.117	8.71	0.131	14.75			0.159	26.76
0.255	8.65	0.154	10.69	0.168	17.58			0.177	28.84
0.279	9.43	0.192	12.76	0.201	20.25			0.194	30.85
0.314	10.52	0.238	15.36	0.202	20.23			0.209	32.56
0.321	10.75	0.266	16.91	0.240	23.20			0.225	34.47
0.354	11.81	0.295	18.50	0.273	25.98				
0.354	11.82	0.336	20.88	0.276	26.15				
0.355	11.83	0.363	22.46	0.281	26.67				
0.388	12.90	0.398	24.47	0.281	26.72				
0.388	12.90	0.398	24.47						
0.422	13.98	0.433	26.61						
0.422	13.98								
0.459	15.13								
0.526	17.21								
0.591	19.32								
0.591	19.26								
0.649	20.99								
0.652	21.23								

$P=10$ atm							
$X=1.322\%$		$X=2.49\%$		$X=5.71$		$X=9.36\%$	
0.027	1.89	0.031	4.75	0.028	15.30	0.034	29.99
0.032	1.98	0.033	4.80	0.034	15.52	0.036	30.12
0.041	2.18	0.044	5.15	0.042	15.92	0.045	30.64
0.062	2.73	0.055	5.67	0.047	16.17	0.056	31.44
0.079	3.22	0.069	6.26	0.054	16.61	0.067	32.40
0.097	3.77	0.079	6.73	0.066	17.45	0.071	32.88
0.131	4.80	0.092	7.39	0.080	18.61	0.085	34.37
0.167	5.94	0.117	8.61	0.090	19.52	0.097	35.81
0.203	7.08	0.155	10.75	0.101	20.54	0.109	37.40
0.243	8.36	0.193	12.85	0.116	21.99		
0.276	9.40	0.240	15.51	0.135	24.01		
0.307	10.42	0.290	18.33	0.155	26.29		
0.361	12.13	0.342	21.34	0.167	27.72		
0.434	14.47	0.398	24.63	0.167	27.71		
0.509	16.84			0.190	30.32		
0.652	21.39			0.202	31.80		
				0.212	33.07		

$P=20$ atm							
$X=1.254\%$		$X=2.34\%$		$X=5.04\%$		$X=7.44\%$	
0.031	1.90	0.028	4.42	0.032	13.37	0.031	22.44
0.031	1.90	0.033	4.55	0.037	13.58	0.037	22.71
0.031	1.91	0.044	4.93	0.042	13.84	0.042	23.04
0.041	2.13	0.044	4.92	0.048	14.26	0.049	23.53
0.062	2.70	0.055	5.40	0.057	14.85	0.057	24.21
0.079	3.22	0.066	5.90	0.063	15.32	0.070	25.51

TABLE I. (Continued)

P = 20 atm							
X = 1.254 %		X = 2.34 %		X = 5.04 %		X = 7.44 %	
T	π	T	π	T	π	T	π
0.095	3.71	0.079	6.55	0.074	16.21	0.082	26.85
0.130	4.78	0.087	6.98	0.085	17.17	0.094	28.23
0.169	6.00	0.117	8.51	0.097	18.38	0.103	29.36
0.204	7.14	0.155	10.65	0.111	19.64	0.103	29.36
0.239	8.29	0.193	12.84	0.129	21.45	0.113	30.75
0.274	9.39	0.238	15.40	0.144	23.00	0.127	32.73
0.304	10.39	0.292	18.52	0.161	24.88	0.141	34.84
0.365	12.33	0.348	21.83	0.176	26.48		
0.438	14.68	0.415	25.81	0.190	28.04		
0.502	16.72			0.203	29.48		
0.651	21.56						

sult of a systematic error in the earlier measurements, specifically a temperature-dependent sensitivity of the strain-gauge pressure transducer (which could not be checked in that experiment). Reanalysis of the earlier data suggests that the values of π at 0.65 and 0.32 K should be reduced by 1% and 3%, respectively. This correction results in a substantial improvement in the agreement between theory and experiment at high temperatures. It also makes the present data at 0.32 K in excellent agreement with the (corrected) earlier data. We have chosen, therefore, to calibrate our transducer against the data of Wilson *et al.*^{3,4} at 0.65 K, reduced by a correction of 1%. This correction was not applied in our earlier paper.¹

III. RESULTS

The results of our measurements of the osmotic pressure for single-phase He³-He⁴ solutions at pressures of 0.26, 10, and 20 atm are shown in

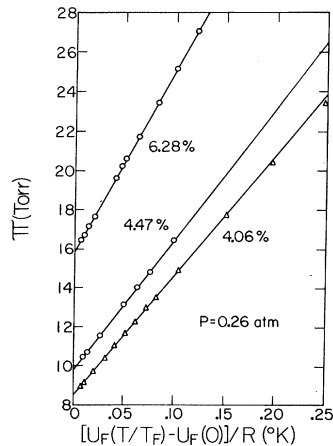


FIG. 3. Some of the osmotic pressure data at 0.26 atm plotted against ΔU_F defined in Eq. (8).

Fig. 2 and listed in Table I. The solid curves through the data are based on a thermodynamic model and will be discussed in Sec. III B. The data points come from two distinct runs, each with independent temperature and transducer calibrations; circles correspond to the first run, squares to the second. One of the remarkable features of these data is the linearity which appears when π is plotted against U_F , the internal energy of an ideal Fermi gas (which is given as a function of T/T_F by Stoner²⁴). In Fig. 3 some of the data at $P = 0.26$ atm are plotted against ΔU_F defined as

$$\Delta U_F = [U_F(T/T_F) - U_F(0)], \quad (8)$$

where T_F is the Fermi temperature [Eq. (2)]. The osmotic pressure at 0 K, $\pi_0(P, X)$, was thus easily obtained by extrapolating to $\Delta U_F = 0$. Our values for $\pi_0(P, X)$ are given in Table II. Values given in parentheses are for concentrations greater than the limiting solubility at that pressure. They were obtained by extrapolating through the two-phase region.

Normally, He³-He⁴ solutions of concentration greater than $X_0(P)$, the solubility at absolute zero, will separate into two phases once the solution passes below its characteristic phase-separation temperature T_s . The upper phase is almost pure

TABLE II. Zero-temperature limit of the single-phase osmotic pressure $\pi_0(X, P)$ for several concentrations and pressures.

P = 0.26 atm		P = 10 atm		P = 20 atm	
X (%)	π_0 (Torr)	X (%)	π_0 (Torr)	X (%)	π_0 (Torr)
1.45	1.72	1.32	1.59	1.25	1.51
2.73	4.58	2.49	4.24	2.34	3.93
4.06	8.35	5.71	14.7	5.04	12.6
4.47	9.60	9.36	29.1	7.44	21.6
6.28	15.5	9.82	(30.7)	8.99	(27.2)
7.14	(18.7)				

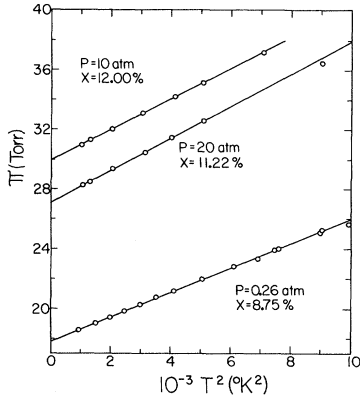


FIG. 4. Osmotic pressure of the lower phase of a phase-separated solution as a function of T^2 .

He^3 at temperatures below 0.2 K, while the concentration of the lower phase decreases gradually with temperature to $X_0(P)$. Our experimental arrangement measures the osmotic pressure of the lower phase $\pi^l(P, T)$ in a phase-separated mixture. We found that $\pi^l(P, T)$ at constant pressure is proportional to T^2 (Fig. 4) in agreement with the observations of London, Phillips, and Thomas.²⁵ Extrapolation to zero temperature gives $\pi_0^l(P)$ which, when plotted on our single-phase graphs of $\pi_0(P)$ versus X , specifies the value of $X_0(P)$. Table III lists our values for π_0^l and X_0 for the pressures studied; these results have been discussed in a previous paper.¹

A. Concentration Dependence of α_0

Using Eq. (5), the values of $\pi_0(P, X)$ deduced from the present data (Table II), and the values of $v_4(P, 0)$ given by Watson,²⁶ we can obtain

$$\mu_4(P, 0, 0) - \mu_4(P, 0, X) = \pi_0(P, X) v_4(P, 0). \quad (9)$$

Table IV lists values of $\pi_0(P, X) v_4(P, 0)$, which quantity is seen to be an extremely weak function of pressure for the concentrations studied. This means that π_0 at zero pressure is only 0.3% less than at 0.26 atm. (Note that the values of π_0 given in a previous paper¹ should be reduced by 1% in view of the calibration adopted in Sec. II.)

TABLE III. Zero-temperature limit of the osmotic pressure of the phase-separated solution π_0^l and the solubility of He^3 in the lower phase X_0 .

$P(\text{atm})$	$\pi_0^l(\text{Torr})$	$X_0(\%)$
0.26	17.7	6.83
0.52	18.6	7.08
5	26.9	8.96
10	29.6	9.52
15	29.0	9.25
20	26.8	8.85

TABLE IV. $\pi_0 v_4/R$ (mK) as a function of pressure at constant X .

$P(\text{atm})$	$X(\%)$			
	3	5	7	9
0.26	2.38	5.07	8.10	...
5	11.4
10	2.34	4.99	7.95	11.2
15	11.1
20	2.28	4.79	7.84	11.0

The variation of $\pi_0(P, X) v_4(P, 0)$ with pressure is related to the variation of the "BBP parameter" $\alpha_0(P, X)$ with concentration. At $T=0$, the molar volume of the solution is

$$v(X, P) = v_4(P, 0) [1 + \alpha_0(X, P) X], \quad (10)$$

and the partial volume of the He^4 in solution is

$$v_4^*(X, P) = v(X, P) - X \frac{\partial v(X, P)}{\partial X}. \quad (11)$$

Expanding $\alpha_0(X, P)$ in powers of X :

$$\alpha_0(X, P) = \alpha_0(P) + \alpha_0'(P) X + \dots, \quad (12)$$

and combining Eqs. (10)–(12), gives

$$v_4^*(X, P) = v_4(P, 0) [1 - \alpha_0'(P) X^2].$$

But $v_4^*(X, P)$ is related to $\mu_4(X, P)$ as

$$v_4^*(X, P) = \left(\frac{\partial \mu_4(X, P)}{\partial P} \right)_{X, T=0},$$

so that

$$\left(\frac{\partial \mu_4(X, P)}{\partial P} \right)_{X, T=0} = v_4(P, 0) [1 - \alpha_0'(P) X^2];$$

Eq. (9) then gives

$$\alpha_0'(P) = \frac{1}{X^2 v_4(P, 0)} \left(\frac{\partial [\pi_0(P, X) v_4(P, 0)]}{\partial P} \right)_{X, T=0}. \quad (13)$$

Using the results in Table IV, we find $\alpha_0'(P) = -(1.1 \pm 0.5) \times 10^{-2}$ independent of pressure and concentration. This result is in striking agreement with the data at $P=0$ of Edwards, Ifft, and Sarwinski²⁷ as shown in Fig. 5, where Eq. (12) has been plotted using $\alpha_0(0) = 0.284$ and $\alpha_0' = -1 \times 10^{-2}$.

Abraham *et al.*²⁸ gave an approximate theoretical expression for the concentration dependence of α_0 based on the BBP result for the He^3 chemical potential. At $T=0$ we have

$$\mu_3 = -E_3 + k_B T_F + n_3 V(0) (1 + \frac{1}{2} F),$$

where $V(0)$ is the $k=0$ value of $V(k)$, and F is the exchange part of the interaction which depends on n_3 and the form of $V(k)$. Making the approximation $F = -1$, corresponding to $V(k) = V(0)$, and assuming $V(0)$ is given by the Baym²⁹ expression

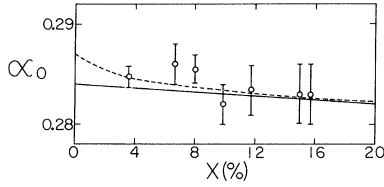


FIG. 5. The "BBP parameter" at 0 K, α_0 , at $P=0$, versus He^3 concentration. Open circles are from Ref. 27. Solid line is Eq. (12) using $\alpha_0(0)=0.284$, with α'_0 determined from the osmotic pressure data. Dashed line is Eq. (15) with $\alpha_0(0)=0.287$.

$$V(0) = -\alpha_0(P)^2 m_4 s^2 / n_4^0, \quad (14)$$

we obtain

$$\begin{aligned} \alpha_0(X, P) \cong \alpha_0(P) &+ \frac{2}{5} \frac{k_B T_F}{m_4 s^2} \left(1 - \frac{3}{2} \frac{\partial \ln m^*}{\partial \ln m_4} \right) \\ &- \frac{X}{2} \alpha_0(P)^2 \left(\frac{\partial \ln s}{\partial \ln m_4} + \frac{\partial \ln \alpha_0}{\partial \ln m_4} \right), \quad (15) \end{aligned}$$

where m_4 is the mass of a He^4 atom and s and n_4^0 are the speed of first sound and number density of pure He^4 at $T=0$, respectively. Equation (15) has been evaluated at $P=0$ using $\partial \ln m^* / \partial \ln m_4$ from Ref. 27, $\partial \ln s / \partial \ln m_4$ and $\partial \ln \alpha_0 / \partial \ln m_4$ from Ref. 26, and $\alpha_0(P)=0.287$. The results are shown as a dashed line in Fig. 5. Once again, the agreement is very good.

B. Temperature Dependence of the Osmotic Pressure

One feature of the present data is the wide range of temperatures studied. A single concentration is measured from the fully degenerate to the semiclassical regime. It is thus possible to compare in detail the predictions of theory with experiment over a wider range of degeneracy than has previously been possible. Unfortunately, this comparison can only be made at $P=0$, where Ebner^{17,18} gave an interaction $V(k)$ suitable for the semiclassical ($T > T_F$) regime. The data from $P=0.26$ atm are reduced to $P=0$ using the empirical fact that πv_4 is very nearly independent of pressure at constant X and T (Sec. III A). The data are further reduced to give the interaction part of π [Eq. (6)] as

$$\pi_{\text{int}} v_4 = \pi(X, T) v_4 - \frac{2}{3} X U_F(T, T_{F0}) - \mu_\alpha, \quad (16)$$

where T_{F0} is the Fermi temperature [Eq. (2)] calculated with the $X \rightarrow 0$ value of the effective mass, m_0^* . Analysis of the $T=0$ data (Sec. III C) gives $m_0^* = 2.23 m_3$ at zero pressure. The internal energy $U_F(T, T_F)$ is given by Stoner²⁴ and has the limits

$$\frac{2}{3} X U_F = \begin{cases} XRT, & T/T_{F0} \gg 1 \\ \frac{2}{5} XRT_{F0}, & T/T_{F0} = 0. \end{cases} \quad (17)$$

The small volume correction μ_α is given by Ebner¹⁸ in the high- and low-temperature limits as

$$\begin{aligned} \mu_\alpha &= \frac{1}{4} X^2 RT_{F0} (1 - \frac{3}{5} \alpha), \quad T/T_{F0} = 0 \\ \mu_\alpha &= \frac{1}{2} X^2 RT (1 - \alpha), \quad T/T_{F0} \gg 1 \end{aligned} \quad (18)$$

and interpolation between these limits was done graphically. The empirical values of $\pi_{\text{int}} v_4$ are shown in Fig. 6 for $X=1.45\%$ and 2.73% . Data for larger values of X are not shown since they are restricted to temperatures less than T_{F0} .

Theoretical values for $\pi_{\text{int}} v_4$ have been computed from the equation given by Ebner¹⁸ for $T > 0.6 T_{F0}$. These are plotted as solid lines in Fig. 6. The squares plotted at $T=0$ in Fig. 6 are calculated from the "optimum" $V(k)$ (Sec. III C) and they determine m_0^* . The agreement of the data and theory is probably as good as one can expect in view of the approximations which have been made. For instance, second-sound experiments¹⁰ indicate that the quasiparticle interaction is a nonlocal potential as proposed by McMillan.³⁰ This could reduce the theoretical values of π_{int} by $\sim 20\%$. The second-sound experiments also indicate that a term proportional to p^4 should be included in the quasiparticle dispersion relation [Eq. (1)]; this effect (which is small) has also been neglected.

At the present time, existing theoretical models do not provide a convenient method for calculating or fitting the temperature dependence of equilibrium properties of solutions, particularly for $T \approx T_F$. In view of this, we have used an empirical thermodynamic model for solutions which is in good

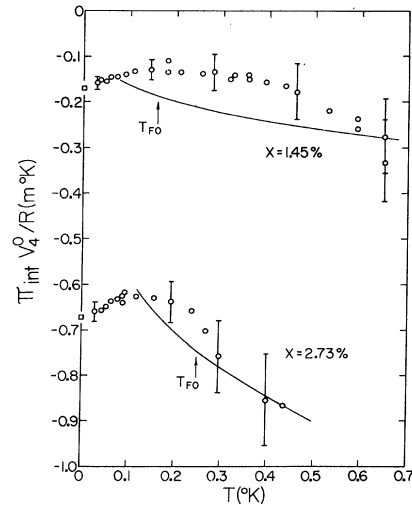


FIG. 6. Contribution to the osmotic pressure at $P=0$ due to the He^3 - He^3 effective potential. Circles are empirical values defined by Eqs. (16)–(18), while curves are theoretical results from Ref. 16. Squares are theoretical results at $T=0$ using $m_0^* = 2.23 m_3$ with the "optimum" potential of Ref. 16.

agreement with the osmotic pressure at all concentrations, temperatures, and pressures, as well as with other equilibrium data. The assumption of the model is that the molar entropy of the mixture is given by

$$S = XS_F(T/T_F) + (1 - X)S_4, \quad (19)$$

where $S_F(T/T_F)$ is the molar entropy of an ideal Fermi gas with an effective mass $m^*(X, P)$ and S_4 is the molar entropy of pure He⁴. The thermodynamic properties of the system are then described in terms of a single empirically determined function $m^*(X, P)$, the specific-heat effective mass. This effective mass should be regarded strictly as an empirical quantity with little or no relation to the inertial effective mass in Eqs. (1) or (16), although as $X \rightarrow 0$, $m^*(X, P)$ should approach $m_0^*(P)$. The proposed model is identical with the assumptions used by Anderson *et al.*⁶ in fitting $m^*(X, P=0)$ from heat-capacity data at $X=1.3$ and 5%. The same model was used by Edwards, Ifft, and Sarwinski²⁷ to explain the thermal expansion of mixtures. The osmotic pressure is obtained from this model by writing the He⁴ chemical potential, at constant T and P , in terms of the Gibbs function per mole of solution G ,

$$\mu_4 = G - X \left(\frac{\partial G}{\partial X} \right)_{T,P}. \quad (20)$$

From Eq. (19) and from the fact that S_F is a function of T/T_F only, we obtain

$$\left(\frac{\partial \mu_4}{\partial T} \right)_{P,X} = S_4 - XC_F \left(\frac{\partial \ln T_F}{\partial \ln X} \right)_P, \quad (21)$$

where C_F is the molar specific heat of an ideal Fermi gas with mass $m^*(X, P)$. Integration of Eq. (21) and the definition of π from Eq. (5) give the temperature dependence of the osmotic pressure as

$$\pi(X, T, P) v_4 = \pi_0(X, P) v_4 + \frac{2}{3} X(1 + \epsilon X) \Delta U_F, \quad (22)$$

where ΔU_F is defined in Eq. (8) and

$$\epsilon = -\alpha - \frac{3}{2} \left(\frac{\partial \ln m^*}{\partial X} \right)_P. \quad (23)$$

This expression for π [Eq. (22)] is similar to one proposed by Varoquaux³¹ based upon a specific empirical form for the He³ chemical potential. Since both expressions are phenomenological, with parameters chosen to fit the data, there is little reason to choose between them. Our expression has the advantage that no integrals over Fermi functions must be evaluated. It should be emphasized that values of $m^*(X, P)$ deduced from data on the basis of these two models will differ.

To simplify the calculations, we introduce the variable ξ , where

TABLE V. Values of parameters used in the empirical thermodynamic fit to the temperature dependence of the osmotic pressure.

$P(\text{atm})$	α	Range	B	A_1	A_2
0.26	0.280	$T < 0.6$	2.57 ± 0.02	-0.37 ± 0.08	-1.13 ± 0.29
		$T < 0.2$	2.46 ± 0.03	0.87 ± 0.29	4.69 ± 0.73
10	0.207	$T < 0.6$	3.06 ± 0.03	-0.12 ± 0.12	-2.46 ± 0.39
		$T < 0.2$	3.03 ± 0.04	0.04 ± 0.27	-2.97 ± 0.75
20	0.176	$T < 0.6$	3.29 ± 0.03	0.28 ± 0.12	-2.90 ± 0.39
		$T < 0.2$	3.26 ± 0.04	-0.32 ± 0.25	-2.69 ± 0.68

$$\xi = \frac{n_3}{n_4} = \frac{X}{1 + \alpha X} \quad (24)$$

and n_4^0 is the number density of pure He⁴ at the same pressure. The concentration dependence of m^* is expressed specifically as

$$m^*(X)/m_3 = B / (1 + A_1 \xi + A_2 \xi^{5/3}). \quad (25)$$

[This has the same form as the BBP expression for the $T \rightarrow 0$ specific-heat mass using a simple parabolic form for $V(k)$.] With these definitions, the expression for π becomes

$$\pi(X, T, P) v_4 = \pi_0(X, P) v_4 + \xi \left(\frac{2}{3} - \frac{\xi}{m^*} \frac{\partial m^*}{\partial \xi} \right) \Delta U_F. \quad (26)$$

A computer was used to perform a weighted least-squares fit of Eqs. (25) and (26) to the data, assuming a standard deviation of 0.4% in π , and allowing m_0^* , B , A_1 , and A_2 to be adjustable parameters. The values of π_0 were obtained from the BBP theory using the formulas and constants described in Sec. III C. The fitted values of m_0^* are discussed in Sec. III C. The weak temperature and concentration dependence of α was neglected; the values of α used in the fit are given in Table V. The fitted values of B , A_1 , and A_2 are listed in Table V. The values of $m^*(X)$ from Eq. (25) are plotted in Fig. 7 for $P=0.26, 10,$ and 20 atm, which indicates that m^* is a very weak function of

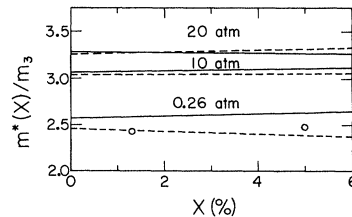


FIG. 7. Specific-heat effective mass versus concentration at three pressures. Solid lines are the result of fitting Eqs. (25) and (26) to the data for all temperatures ($T \leq 0.65$ K). The dashed lines are for data restricted to $T \leq 0.2$ K. The open circles at $P=0.26$ atm result from a least-squares fit of the heat-capacity data ($T \leq 0.2$ K) of Ref. 6.

TABLE VI. The specific-heat effective mass from various sources.

Source	$\frac{m^*}{m_3}$ (1.3%)	$\frac{m^*}{m_3}$ (5%)
Specific-heat data (Ref. 6)	2.38 ± 0.04	2.46 ± 0.04
Data of Ref. 6 refitted	2.42 ± 0.04	2.47 ± 0.04
Osmotic pressure $T < 0.65$ K reduced to $P=0$	2.58 ± 0.03	2.62 ± 0.03
Osmotic pressure $T < 0.2$ K reduced to $P=0$	2.46 ± 0.04	2.39 ± 0.04

concentration. The values of $m^*(X)$ for $P=0.26$ atm when reduced to $P=0$ using $\partial \ln m^*/\partial P = 1.5 \times 10^{-2} \text{ atm}^{-1}$ (Ref. 27) disagree with the values deduced by Anderson *et al.*,⁶ from specific-heat measurements. The values are compared in Table VI, which includes the results of applying our least-squares fitting program to recalculate m^* from the specific heats of Anderson *et al.*,⁶ assigning a standard deviation of 1% to the data points. The disagreement is removed if we fit only the π data for $T \leq 0.2$ K (the same range of T in which the specific heat was measured). The $m^*(X)$ which results from this fit is also shown in Fig. 7. The fact that $m^*(X)$ depends on the range of T indicates that the model is not a perfect fit to the data, but on the other hand it is very satisfactory as shown by the solid lines in Fig. 2. At all three pressures, the calculated values of π typically disagree by less than 1% with the measured values. The model therefore provides a convenient framework for computing equilibrium properties of solutions and examining the consistency of various thermodynamic data.

C. Pressure Dependence of the Potential $V(k)$

The results of Sec. III B indicate that analysis of the temperature dependence of π is unlikely to be helpful in obtaining the He³ quasiparticle scattering potential $V(k)$. At $T=0$, however, the interaction contribution to π_0 is¹⁸

$$\pi_{\text{int}} = \frac{1}{2} n_3^2 V(0) - \frac{3n_3^2}{(2k_F)^4} \int_0^{2k_F} \left(1 - \frac{k^2}{4k_F^2}\right) V(k) k^3 dk, \quad (27)$$

where

$$k_F = (3\pi^2 n_3)^{1/3} \quad (28)$$

so that $V(k)$ may in principle be determined from the n_3 dependence of π_{int} . Reduction of the data to obtain π_{int} requires [Eq. (16)] values for the $X \rightarrow 0$ value of the inertial effective mass m_0^* . With some loss of precision, it is also possible to determine m_0^* as well as $V(k)$ from π_0 .

We first consider the situation at low pressure, where Ebner¹⁶ has given an "optimum" $V(k)$ determined by the low-temperature transport properties of solutions. He assumed that the potential could be expanded in powers of k^2 as

$$V(k) = V_0 [a_0 + a_1 y + a_2 y^2 + a_3 y^3 + a_4 y^4], \quad (29)$$

where $y = (k/2k_0)^2$, the momentum $k_0 = 0.318 \text{ \AA}^{-1}$, and

$$n_4^0(P=0) V_0/k_B = -2.13 \text{ K}.$$

The parameters a_0, a_1, a_2, a_3 , and a_4 were then chosen by fitting the experimental transport data and requiring that $V(k)$ be only "reasonably rapidly varying." The resulting parameters given by Ebner are shown in Table VII.

Substituting Eq. (29) into (27) gives

$$\pi_{\text{int}} = \frac{1}{4} n_4^0 \xi^2 (n_4^0 V_0) \left[a_0 - \frac{1}{2} a_1 y_F - \frac{3}{10} a_2 y_F^2 - \frac{1}{5} a_3 y_F^3 - \frac{1}{7} a_4 y_F^4 \right], \quad (30)$$

where $y_F = (k_F/k_0)^2$. Using the Ebner parameters in Eq. (30) and $m_0^* = 2.34 m_3$, we previously¹ compared the theoretical π_0 with the experimental osmotic pressure extrapolated to zero temperature and pressure. The results indicated a 10–20% disagreement in π_{int} .

As described in Sec. III B, we now have an alternative (and better) procedure to compare the osmotic pressure with theory. In fitting the data at finite temperatures and 0.26 atm to Eq. (26), π_0 was determined by the BBP formula with an adjustable m_0^* and the Ebner "optimum" potential

TABLE VII. Values of constants in a speculative He³ quasiparticle potential of the form $V(k) = V_0 [a_0 + a_1 y + a_2 y^2 + a_3 y^3 + a_4 y^4]$ and of the inertial effective mass m_0^* used to fit the zero-temperature osmotic pressure at various pressures.

$P(\text{atm})$	a_0	a_1	a_2	a_3	a_4	$\frac{m_0^*}{m_3}$	$\frac{n_4^0(P) V(0)}{k_B} (\text{K})$	m_0/m_3 (Second sound, Ref. 10)	$(-a^2 m_4 s^2/k_B) (\text{K})$ [Baym formula, Eq. (14)]
0.26	1	-3.389	+6.353	-9.576	+5.402	2.24	-2.13	2.28 ± 0.03	-2.05
10	0.700	+3.822	-19.89	+24.90	-9.528	2.72	-1.62	2.57 ± 0.04	-1.91
20	0.600	+6.314	-30.50	+38.28	-14.69	2.93	-1.49	2.85 ± 0.04	-1.81

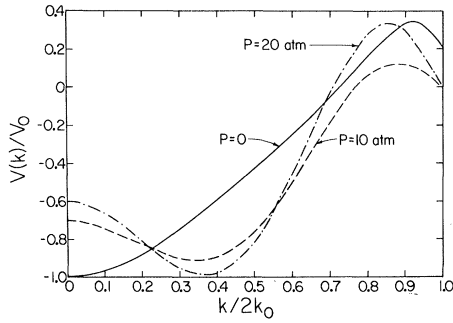


FIG. 8. Some He^3 quasiparticle effective potentials, $V(k)$ deduced from the $T=0$ osmotic pressure at $P=0$, 10, and 20 atm. Parameters of the potential [Eq. (29)] and values of the inertial effective mass m_0^* are given in Table VII.

[Eq. (29)]. It is found that $\pi(X, T)$ can be fitted within a root-mean-square deviation of 0.7% with $m_0^* = (2.24 \pm 0.03)m_3$, in good agreement with the results of recent second-sound measurements,¹⁰ $(2.27 \pm 0.03)m_3$. Allowing for the fact that the true potential is probably nonlocal^{10,30} would improve this agreement. Thus, we have an excellent fit to the theory at 0 K using Ebner's "optimum" potential. The values of π_0 from the fit are within 1% of the extrapolated values.

Analysis of the data at 10 and 20 atm proceeded somewhat differently since $V(k)$ was not known at all at elevated pressures. Baym²⁹ gave an equation for the $k=0$ value of the potential [Eq. (14)]:

$$V(0) = -\alpha^2 m_4 s^2 / n_4^0, \quad (14)$$

where m_4 is the mass of a He^4 atom and s and n_4^0 are the speed of first sound and the number density in pure He^4 at $T=0$, respectively. With the same fitting procedure used to evaluate the potential parameters from the transport data, Ebner (private communication) determined $V(k)$ and m_0^* from π_0 at 10- and 20-atm pressure. [Note that, including m_0^* , there are six adjustable parameters to be determined while, under pressure, there are only four concentrations to be fitted. The fit was made unique by requiring that the $V(k)$ be "only reasonably rapidly varying."¹⁶] At 10 atm, π_{int} could be fitted to $\sim 1\%$ and at 20 atm to $\sim 5\%$. The potential parameters and m_0^* are given in Table VII and the potentials are plotted in Fig. 8 along with the $P=0$ potential.

The values of m_0^* inferred from fitting the osmotic pressure should be compared with the values determined from preliminary second-sound results¹⁰ also shown in Table VII. The magnitudes of $V(0)$ at 10 and 20 atm are given in the Table along with values calculated²⁶ from the Baym expression [Eq. (14)]. The agreement is fair. It is interesting to note that the minimum $V(k)$ no longer

occurs at $k=0$ at 10 and 20 atm. This implies a much higher "supermobile" transition temperature ($\sim 10^{-4}$ K) for solutions under pressure. The procedure to find $V(k)$ by fitting π_0 is somewhat arbitrary and is rather sensitive to the values of m_0^* . Given the discrepancy with the second-sound masses, the neglect of nonlocal effects in the potential, and of p^4 terms in the dispersion relation, we can only regard the potentials shown in Fig. 8 as highly speculative. They are presented in this paper only to show that the "supermobile" transition temperature may increase with pressure, although $V(0)$ becomes less attractive, in agreement with Eq. (14).

IV. CONCLUSIONS

The extensive amount of thermodynamic information obtained from the osmotic pressure data has made possible a fairly critical comparison with theory. In particular, the effects of temperature and pressure can be analyzed in more detail than was previously possible.

The limiting case of $P=0$ and $T=0$ has been the subject of the majority of earlier work on solutions, both experimental and theoretical. In this case we find that the local He^3 quasiparticle potential determined from transport data is in excellent agreement with the osmotic pressure when the effective inertial mass at $X=0$ is taken to be $m_0^* = 2.23m_3$. This value of m_0^* is also in fair agreement with the value deduced from second-sound data.

For elevated pressures at $T=0$, the osmotic pressure data suggest that the potential may differ qualitatively from that at $P=0$, implying a much higher "supermobile" transition temperature. The availability of transport data at elevated pressures would clearly be useful. Extension of the microscopic theory³² to include the higher density systems should also prove quite interesting.

Comparison with theory for $T>0$ is rather difficult and imprecise although, at least for $P=0$, the situation appears more hopeful than had been thought earlier.³ Rather than attempt a complicated fitting of the temperature dependence to some $V(k)$, we chose to examine the empirical thermodynamic model used to analyze the specific-heat data. We find that a specific-heat effective mass $m^*(X, P)$ can be chosen to give an excellent fit to the osmotic pressure. The results provide a convenient empirical framework for the calculation of the thermodynamic properties of solutions.

ACKNOWLEDGMENTS

We are extremely grateful to Dr. C. Ebner for his work with the computer programs and for his many helpful discussions about interpretation of the data, and to Dr. R. Sherlock for the results of analysis of the second-sound data.

- *Work supported by the National Science Foundation.
- ¹J. Landau, J. T. Tough, N. R. Brubaker, and D. O. Edwards, *Phys. Rev. Letters* **23**, 283 (1969).
- ²A. Ghazlan, P. Piejus, and E. Varoquax, *C. R. Acad. Sci. Paris, Ser. B* **269**, 344 (1969).
- ³M. F. Wilson, D. O. Edwards, and J. T. Tough, *Phys. Rev. Letters* **19**, 1368 (1967).
- ⁴M. F. Wilson and J. T. Tough, *Phys. Rev. A* **1**, 914 (1970).
- ⁵L. D. Landau and I. Pomeranchuk, *Dokl. Akad. Nauk SSSR* **59**, 669 (1948).
- ⁶A. C. Anderson, D. O. Edwards, W. R. Roach, R. E. Sarwinski, and J. C. Wheatley, *Phys. Rev. Letters* **17**, 367 (1966).
- ⁷C. G. Niels-Hakkenberg, L. Meermans, and H. C. Kramers, in *Proceedings of the Eighth International Conference on Low-Temperature Physics, London, 1962*, edited by R. O. Davies (Butterworths, London, 1963), p. 45.
- ⁸D. J. Sandiford and H. A. Fairbank, *Phys. Rev.* **162**, 192 (1967).
- ⁹P. V. E. McClintock, K. H. Mueller, R. A. Guyer, and H. A. Fairbank, in *Proceedings of the Eleventh International Conference of Low Temperature Physics*, edited by J. F. Allen, D. M. Finlayson, and D. M. McCall, St. Andrews, Scotland, 1968 (University of St. Andrews Printing Department, St. Andrews, Scotland, 1969), p. 379.
- ¹⁰N. R. Brubaker, D. O. Edwards, R. E. Sarwinski, P. Seligman, and R. A. Sherlock, *Phys. Rev. Letters* **25**, 714 (1970).
- ¹¹P. Seligmann, D. O. Edwards, R. E. Sarwinski, and J. T. Tough, *Phys. Rev.* **181**, 415 (1969).
- ¹²L. D. Landau and E. M. Lifshitz, *Statistical Physics* (Addison-Wesley, Reading, Mass., 1958).
- ¹³J. Bardeen, G. Baym, and D. Pines, *Phys. Rev.* **156**, 207 (1967).
- ¹⁴W. R. Abel, R. T. Johnson, J. C. Wheatley, and W. Zimmerman, Jr., *Phys. Rev. Letters* **18**, 737 (1967).
- ¹⁵G. Baym and C. Ebner, *Phys. Rev.* **170**, 346 (1968).
- ¹⁶C. Ebner, *Phys. Rev.* **185**, 392 (1969).
- ¹⁷C. Ebner, *Phys. Rev.* **156**, 222 (1967).
- ¹⁸C. Ebner, Ph.D. thesis, University of Illinois, 1967 (unpublished).
- ¹⁹Epibond Epoxies are manufactured by Furane Plastics, Inc., 4576 Brazil St., Los Angeles, Calif.
- ²⁰M. F. Wilson, D. O. Edwards, and J. T. Tough, *Rev. Sci. Instr.* **39**, 134 (1968).
- ²¹J. Landau, J. T. Tough, N. R. Brubaker, and D. O. Edwards, *Rev. Sci. Instr.* **41**, 444 (1970).
- ²²R. I. Boughton, Jr., N. R. Brubaker, and R. E. Sarwinski, *Rev. Sci. Instr.* **38**, 1177 (1967).
- ²³R. P. Hudson, *Cryogenics* **4**, 76 (1969).
- ²⁴E. C. Stoner, *Phil. Mag.* **25**, 901 (1938).
- ²⁵H. London, D. Phillips, and G. P. Thomas, in *Ref. 9*, p. 649.
- ²⁶G. E. Watson, Ph.D. thesis, Cornell University, 1969 (unpublished); G. E. Watson, J. D. Reppy, and R. C. Richardson, *Phys. Rev.* **188**, 384 (1969).
- ²⁷D. O. Edwards, E. M. Ifft, and R. E. Sarwinski, *Phys. Rev.* **177**, 380 (1969).
- ²⁸B. M. Abraham, O. G. Brandt, Y. Eckstein, J. Munarin, and G. Baym, *Phys. Rev.* **188**, 309 (1969).
- ²⁹G. Baym, *Phys. Rev. Letters* **17**, 952 (1966).
- ³⁰W. L. McMillan, *Phys. Rev.* **175**, 266 (1968); **182**, 299 (1969).
- ³¹E. Varoquax, *C. R. Acad. Sci. Paris, Ser. B* **266**, 893 (1968).
- ³²C-W Woo, H-T Tan, and W. E. Massey, *Phys. Rev. Letters* **22**, 278 (1969); *Phys. Rev.* **185**, 287 (1969); *ibid.* (to be published).

Fluctuations and Light Scattering in Cholesteric Liquid Crystals*

Chungpeng Fan, Lorenz Kramer, and Michael J. Stephen

Physics Department, Rutgers University, New Brunswick, New Jersey 08903

(Received 3 June 1970)

The normal modes of an incompressible cholesteric liquid crystal are determined from the hydrodynamical equations. There are two important modes which should be readily observable by light scattering. The first mode is a twisting and untwisting of the helical structure. The second mode is a combination viscous-splay mode. Both modes are overdamped. These modes scatter light most strongly for momentum transfers exactly equal to and exactly one-half of those leading to Bragg scattering, respectively. Thus the modes should be easily separated experimentally. The normal modes are also evaluated in the presence of a transverse magnetic field, and the damping constants turn out to be quite sensitive functions of the magnetic field.

I. INTRODUCTION

Cholesteric liquid crystals are composed of optically active molecules which in many cases are derivatives of cholesterol.¹ The long axes of the molecules tend to be in planes, and in any plane the

ordering is like that in a nematic liquid crystal, i. e., the molecular axes tend to be parallel. However, the structure is probably not a layered one. In a direction perpendicular to these planes the axes are rotated from one point to another, and thus the